AAS 19-266

DESIGNING LOW-THRUST ENABLED TRAJECTORIES FOR A HELIOPHYSICS SMALLSAT MISSION TO SUN-EARTH L5

Ian Elliott[*], Christoper Sullivan Jr.[*], Natasha Bosanac[†], Jeffrey R. Stuart[‡], and Farah Alibay[§]

A small satellite deployed to Sun-Earth L5 could serve as a low-cost platform to observe solar phenomena such as coronal mass ejections. However, the small satellite platform introduces significant challenges into the trajectory design process via limited thrusting capabilities, power and operational constraints, and fixed deployment conditions. To address these challenges, a strategy employing dynamical systems theory is used to design a low-thrust-enabled trajectory for a small satellite to reach the Sun-Earth L5 region. This procedure is demonstrated for a small satellite that launches as a secondary payload with a larger spacecraft destined for a Sun-Earth L2 halo orbit.

INTRODUCTION

Low-thrust spacecraft trajectory design has the potential to enable targeted science missions for small satellites to explore solar processes. In fact, the Sun-Earth (SE) L5 equilibrium point, located at the vertex of an equilateral triangle formed with the Sun and the Earth, is a candidate for locating a SmallSat for a heliophysics mission. At SE L5, a spacecraft would have a currently unavailable perspective of the three-dimensional structure of the coronal mass ejections off the Sun-Earth line.[1] Additionally, due to the rotation of the Sun, early warning of solar storms is possible from SE L5.[2] This equilibrium point has previously been visited by the Solar TErrestrial RElations Observatory B (STEREO-B) spacecraft which drifted through the SE L5 region, but did not maintain long-term bounded motion.[3,4] With the increasing availability of rideshare opportunities and the recent demonstration of CubeSats operations in deep space during the Mars Cube One (MarCO) mission,[5] small satellites may soon have the potential to be deployed to SE L5 to perform heliophysics-based science objectives.

While small satellites have emerged as a low-cost option for performing on-orbit science, their form factor introduces several challenges into the trajectory design process. These challenges include constrained deployment conditions due to their status as a secondary payload as well as limited operational capabilities such as available thrust, propellant mass, and power generation.[6] In this work, the trajectory design process is demonstrated for two spacecraft models that represent

[*]Graduate Research Assistant, Smead Department of Aerospace Engineering Sciences, University of Colorado Boulder, Boulder CO, 80309

[†]Assistant Professor, Colorado Center for Astrodynamics Research, Smead Department of Aerospace Engineering Sciences, University of Colorado Boulder, Boulder CO, 80309

[‡]Mission Design and Navigation Systems Engineer, Jet Propulsion Laboratory, California Institute of Technology, Pasadena CA, 91109

[§]Systems Engineer, Jet Propulsion Laboratory, California Institute of Technology, Pasadena CA, 91109

the upper and lower capabilities of the small satellite form factor.[7] At the lower capability end of the small satellite class is a 6U CubeSat equipped with a low-thrust electrospray engine, which is currently in development for CubeSats as a modular, commercial off-the-shelf propulsion system.[8] An ESPA-class SmallSat with a Hall-effect thruster is considered as the current high-performance extreme of the small satellite class.[7] The development of a trajectory design procedure that can accommodate form factors between these two extremes, the properties of low-thrust propulsion systems and driving constraints can enable rapid small satellite mission concept development.

To design complex, low-thrust-enabled trajectories that are feasible – subject to the constraints associated with small satellite missions – dynamical systems techniques are useful.[9] First, the dynamics of a spacecraft within the Sun-Earth system are approximated using the autonomous Circular Restricted Three-Body Problem (CR3BP). In this model, fundamental natural dynamical structures exist, including: equilibrium points, periodic orbits, quasi-periodic and manifolds. Analysis of these natural motions offers insight into the design of efficient low-thrust trajectories within multi-body systems. In particular, constants of motion and their associated bounds on feasible motion guide the design of itineraries and heuristic thrusting strategies. Furthermore, arcs along natural structures are assembled and connected via low-thrust segments to form a reasonable initial guess for an end-to-end trajectory. In the Sun-Earth system, these structures tend to reflect the geometry of motions that exist in high fidelity ephemeris models. To effectively transition a discontinuous initial guess, assembled in the CR3BP, to a point mass ephemeris model of the Sun-Earth-Moon system, a multiple shooting corrections strategy is used. This general procedure is outlined, improving upon previous work by Bosanac, Alibay and Stuart.[7] This approach is then applied to the design of a low-thrust trajectory for a SmallSat and CubeSat spacecraft model to Sun-Earth L5. The presented results demonstrate the use of dynamical systems theory to enable the design of low-thrust-enabled trajectories with limited required propulsive effort and subject to a variety of mission constraints.

SPACECRAFT MODELS

To develop a low-thrust enabled trajectory, the baseline spacecraft configurations and associated propulsion systems must first be defined. To capture the variety of characteristics for spacecraft in the small satellite family, two spacecraft models are leveraged based on current technological capabilities.[7] First, an ESPA-class SmallSat represents small satellites with a high available thrust and specific impulse, I_{sp}, corresponding to a Hall-effect thruster.[10] A 6U CubeSat model is used to represent lower performance spacecraft, with lower available thrust and lower specific impulse, based on the characteristics of an electrospray engine.[11] Table 1 summarizes both spacecraft models and associated parameters used in this study, using quantities first presented by Bosanac, Alibay and Stuart.[7]

Table 1. Characteristics of baseline spacecraft configurations.

Parameter	6U CubeSat[11]	ESPA SmallSat[10]
Available Thrust (mN)	0.4	13
I_{sp} (s)	1250	1375
Wet Mass (kg)	14	180
Available Propulsion Power (W)	10	200

DYNAMICAL MODELS

Models of increasing fidelity are leveraged in a dynamical systems approach to designing a complex path for a small satellite in a multi-body system, subject to a variety of constraints. Initially employing the lower-fidelity CR3BP, where possible, guides the trajectory design process via rapid and informed analysis of natural dynamical structures. Arcs selected from these structures to satisfy the mission constraints are then assembled and combined with low-thrust segments to create an initial guess with a desired geometry. This discontinuous guess is then transitioned to a higher-fidelity point mass ephemeris model and corrected for continuity. This approach of gradually increasing the model fidelity reduces the computational complexity and effort required to identify feasible yet constrained transfers for small satellites during mission concept development.

Circular Restricted Three-Body Problem

In the multi-body gravitational environment of the Sun-Earth system, the CR3BP offers a useful approximation of the nonlinear and chaotic dynamics of an assumed massless particle, P_3. The CR3BP approximates the motion of two primary bodies – the Sun, P_1, and the Earth, P_2 – via circular orbits about the mutual barycenter.[12] A Sun-Earth rotating frame, $\hat{x}\hat{y}\hat{z}$, is defined to rotate with the primary bodies, such that P_1 and P_2 are fixed along the horizontal $\hat{x}$ axis for all time. The $\hat{z}$ axis is defined in the direction of the angular velocity of the system, while the $\hat{y}$ axis completes the right-handed coordinate frame. This rotating frame is displayed in Figure 1 relative to the inertial frame, $\hat{X}\hat{Y}\hat{Z}$. Next, nondimensionalization of mass, length, and time quantities is performed using the total mass of the system, the distance between P_1 and P_2, and the mean motion of the primaries. Then, the system mass ratio μ is defined as the ratio $\mu = m_2/(m_1 + m_2)$ where m_1 and m_2 are the masses of the primary bodies and $m_2 \leq m_1$. In the Sun-Earth system, the mass ratio possess a value of approximately $\mu \approx 3.0035 \times 10^{-6}$. Then, a nondimensional state vector, $\vec{x} = [x, y, z, \dot{x}, \dot{y}, \dot{z}]^T$, describes the state of P_3 in the rotating frame relative to the system's barycenter. Using these

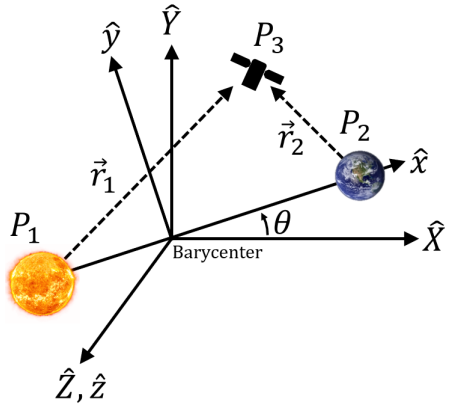

Figure 1. Definition of the Sun-Earth rotating frame, $\hat{x}\hat{y}\hat{z}$, relative to an inertial frame, $\hat{X}\hat{Y}\hat{Z}$.

definitions, the nondimensional equations of motion in the rotating frame are then written as:

$$\begin{aligned}\ddot{x} &= 2\dot{y} + x - \frac{(1-\mu)(x+\mu)}{r_1^3} - \frac{\mu(x-1+\mu)}{r_2^3} \\ \ddot{y} &= -2\dot{x} + y - \frac{(1-\mu)y}{r_1^3} - \frac{\mu y}{r_2^3} \\ \ddot{z} &= -\frac{(1-\mu)z}{r_1^3} - \frac{\mu z}{r_2^3}\end{aligned} \tag{1}$$

where $r_1 = \sqrt{(x+\mu)^2 + y^2 + z^2}$ and $r_2 = \sqrt{(x-1+\mu)^2 + y^2 + z^2}$ are the distances of P_3 from P_1 and P_2, respectively. This dynamical system is nonlinear and chaotic, admitting a large variety of solutions.

Within the CR3BP, and at a fixed mass ratio, five equilibrium points exist, representing constant solutions in the rotating frame. These five equilibrium points include the collinear equilibrium points (L1, L2, L3) and the triangular equilibrium points (L4, L5). The collinear equilibrium points lie along the $\hat{x}$ axis of the rotating frame while the triangular equilibrium points form an equilateral triangle with the primary bodies in the xy-plane of the rotating frame.

In the CR3BP, an integral of motion exists in the rotating frame. In fact, the Jacobi constant, C_J, is a energy-like constant for natural trajectories in the CR3BP, defined as:

$$C_J = 2U^* - (\dot{x}^2 + \dot{y}^2 + \dot{z}^2) \tag{2}$$

where U^* is a pseudo-potential term defined as:

$$U^* = \frac{1}{2}(x^2 + y^2) + \frac{1-\mu}{r_1} + \frac{\mu}{r_2} \tag{3}$$

Using this definition, a low value of the Jacobi constant is analogous to a higher energy for P_3 as it moves within the multi-body system. Although the Jacobi constant is only conserved in the CR3BP, and not in any higher fidelity models, it is valuable in preliminary trajectory design activities.

Low-Thrust Enabled Point Mass Ephemeris Model

A low-thrust enabled point-mass ephemeris model is constructed using information about celestial bodies available through NASA's SPICE toolkit.[13] The forces assumed to act on the spacecraft in this dynamical system include the gravitational effects of point mass models of the Sun, Earth and Moon as well as a propulsive force, $\vec{F}_{lt}$, due to a low-thrust engine. To formulate the equations of motion, the mass of the spacecraft is considered to have a negligible gravitational effect on the primary bodies. Then, the spacecraft is described by a state vector, $\vec{X} = [X, Y, Z, \dot{X}, \dot{Y}, \dot{Z}]^T$, defined in a Earth-centered inertial frame and nondimensionalized using the same characteristic quantities as in the CR3BP.[14] Using these definitions, the nondimensional equations of motion for the spacecraft in the inertial frame are written as:

$$\ddot{\vec{R}}_{E,sc} = G\left[-m_E\left(\frac{\vec{R}_{E,sc}}{R_{E,sc}^3}\right) + m_S\left(\frac{\vec{R}_{sc,S}}{R_{sc,S}^3} - \frac{\vec{R}_{E,S}}{R_{E,S}^3}\right) + m_M\left(\frac{\vec{R}_{sc,M}}{R_{sc,M}^3} - \frac{\vec{R}_{E,M}}{R_{E,M}^3}\right)\right] + \frac{F_{lt}}{m_{sc}}\hat{u} \tag{4}$$

where G is the nondimensionalized gravitational constant, m is mass, and the subscript sc indicates the spacecraft, E the Earth, S the Sun, and M the Moon.[14] The relative vector $\vec{R}_{E,sc}$, locating the spacecraft with respect to the Earth, is defined as

$$\vec{R}_{E,sc} = \vec{R}_{sc} - \vec{R}_E \tag{5}$$

The thrust direction $\hat{u}$ is defined in the spacecraft's velocity, normal, co-normal (VNC) frame with respect to the Earth and then transformed to the inertial frame. Additional external perturbations, such as solar radiation pressure and J_2, are not currently considered. When incorporating the effects of a low-thrust engine, the spacecraft's mass loss due to propellant usage is calculated using the mass flow rate equation. Assuming constant thrust, F_{lt}, and a constant I_{sp}, this equation is written as:

$$\dot{m}_{sc} = -\frac{F_{lt}}{I_{sp}\, g_0} \tag{6}$$

where g_0 is the gravitational acceleration measured at the surface of the Earth, $g_0 = 9.81$ m/s.

INSIGHTS FROM DYNAMICAL SYSTEMS THEORY

Natural Dynamical Structures

The CR3BP admits a large variety of fundamental solutions that are useful in generating an initial guess for a complex trajectory in the Sun-Earth system. Specifically, equilibrium points, periodic orbit families, and invariant manifolds tend to guide the flow within a system modeled by the CR3BP – and are approximately retained in a high fidelity model. At a system mass ratio equal to that of the Sun-Earth system, the collinear equilibrium points (L1, L2, and L3), are unstable equilibria, admitting stable and unstable manifolds that flow between various regions of the system.[15] In the CR3BP, the Jacobi constant enables computation of theoretically reachable or allowable regions of motion for a spacecraft in the CR3BP. The boundary between the reachable and forbidden regions of space are known as zero-velocity surfaces; their intersection with the xy plane produces zero-velocity curves (ZVCs). As the Jacobi constant is decreased below the values of the Jacobi constant corresponding to L1 and L2, the ZVCs define "gateways" around the equilibrium points.[16] For instance, for a spacecraft to depart the vicinity of the secondary body, i.e., the Earth, it must pass through either the L1 or L2 gateway. Figure 2 displays two set of ZVCs in a Sun-Earth rotating frame using dimensional coordinates. Gray shaded regions correspond to regions of forbidden motion where a spacecraft cannot be located for a given value of the Jacobi constant in the CR3BP. White regions in the figure represent locations in the xy plane where a spacecraft can travel naturally. Then, equilibrium points are displayed as red diamonds. In Figure 2(a), the ZVCs are computed at a value of the Jacobi constant higher than the Jacobi constant value of both L1 and L2. For this case, both the L1 and L2 gateways are closed, preventing motion from departing Earth vicinity. In fact, a maneuver that increases the energy of the spacecraft would be required to lower the Jacobi constant and open the gateways to resemble Figure 2(b). In this figure, motion is free to travel towards or away from Earth vicinity. Such analysis using the ZVCs – and the zero velocity surfaces – offers useful insight into a variety of preliminary trajectory design activities such as itinerary design and the development of heuristics for initial maneuver planning.

In the trajectory design process leveraged in this analysis, families of periodic orbits in the vicinity of the equilibrium points are valuable for mission orbit selection. In particular, the L4 and L5 periodic orbit families contain stable orbits useful for performing science over long time intervals – and are approximately retained in a point mass ephemeris model.[15] Furthermore, many members of the Lyapunov, halo, and vertical periodic orbit families near L1, L2, and L3, admit invariant manifolds that capture the flow of natural motion towards or away from the orbit.[17] These stable and unstable manifolds govern the existence and characteristics of natural and low-cost transfers within the system. Examining the unstable manifolds emanating from the L2 periodic orbit families

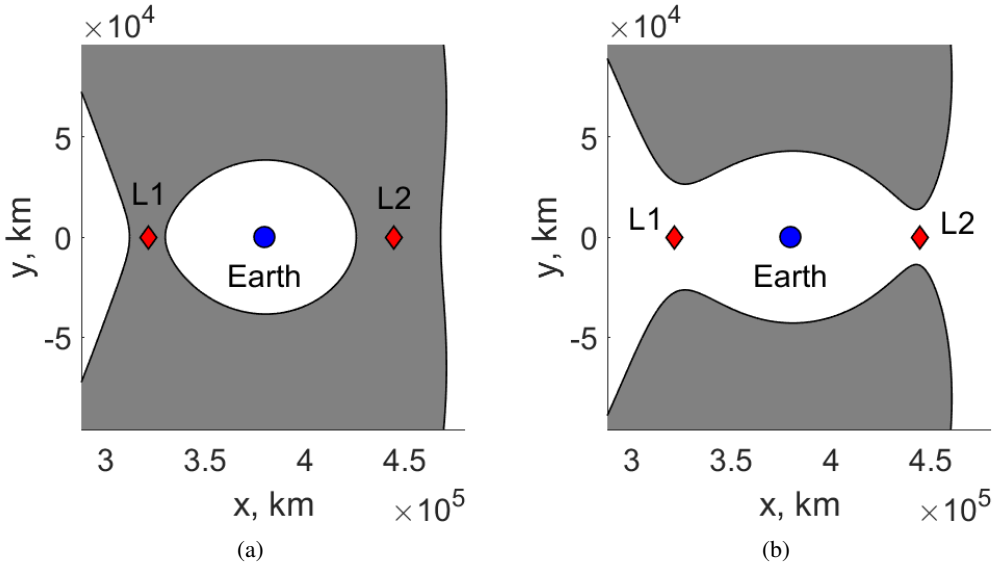

Figure 2. Zero velocity curves in the Sun-Earth CR3BP for (a) $C_J(L_2) < C_J(L_1) < C_J$ and (b) $C_J < C_J(L_2) < C_J(L_1)$

reveal that motion along an unstable manifold will naturally travel towards the vicinity of L5. Similarly, motion that departs along an unstable manifold of an L1 orbit naturally approaches the L4 region. This straightforward insight into natural flow mechanisms indicates that a predominantly natural transfer from the SE L2 gateway to SE L5 may be constructed using the unstable manifolds associated with periodic orbits in the SE L2 neighborhood.

Poincaré Mapping

To enable the informed selection of individual segments when assembling an initial guess, Poincaré maps are useful. This strategy involves capturing the intersection of many trajectories with a hyperplane selected by the mission designer, e.g., at a fixed value of a coordinate in the rotating frame or at an apse.[18] Representation of these intersections on a map supports selection of arcs with favorable characteristics, such as desired flight times or Jacobi constant, for use during initial guess construction.[9] Specifically, selecting arcs that intersect the hyperplane with similar states enables construction of an initial guess with small discontinuities - potentially biasing the corrections algorithm towards a nearby, smooth solution.

TRAJECTORY CORRECTIONS

To recover a continuous trajectory in the point mass ephemeris model from a discontinuous initial guess, a multiple shooting corrections algorithm is employed.[19] A conceptual representation of the multiple shooting corrections process is displayed in Figure 3, with coast arcs colored blue and low-thrust arcs in red. The general procedure for a multiple shooting algorithm begins by discretizing the initial guess trajectory into a sequence of N arcs. A node located at the beginning of the i-th arc, described by the state, $\bar{x}(t_i)$, at time, t_i, is integrated forward for a time Δt_i. All N nodes and associated integration times, as well as any additional variables, are then simultaneously adjusted in an iterative manner via Newton's method to achieve continuity between neighboring arcs. Through this computational approach, relying on discretizing the path into multiple arcs, the sensitivity of the

problem is significantly reduced. Furthermore, a multiple shooting formulation supports enforcing connectivity between both natural coasting arcs and low-thrust segments in both the CR3BP and point mass ephemeris models. While a multiple shooting algorithm does not optimize any objective functions, it is a powerful tool for finding continuous trajectories that retains the general structure of the nearby initial guess. To implement the described multiple shooting algorithm, a free variable and constraint formulation is employed.[14]

A free variable vector, $\vec{V}$, is constructed to reflect the variables describing each arc along the solution. This free variable vector is formed by combining the individual vectors $\vec{V}_i$ describing each arc for $i = 1, \ldots, N$. If the i-th arc corresponds to a natural solution, $\vec{V}_i$ is written as:

$$\vec{V}_i = \begin{bmatrix} \vec{X}_{i,0}^T & m_{i,0} & T_i & \Delta t_i & \beta_i \end{bmatrix}^T \tag{7}$$

where $\vec{X}_{i,0}$ is the nondimensional state of the node at the beginning of the arc in the Earth-centered inertial frame, $m_{i,0}$ is the initial mass of the spacecraft in kg, T_i is the nondimensional time at the beginning of the arc measured from the initial epoch at deployment and Δt_i is the nondimensional integration time along the arc.[19] In addition, β_i is a slack variable used to ensure a positive integration time along the i-th arc. If, however, the i-th arc is generated with a low-thrust maneuver in a direction that is constant along the entire arc and in the VNC frame $\vec{V}_i$ is defined as:

$$\vec{V}_i = \begin{bmatrix} \vec{X}_{i,0}^T & m_{i,0} & T_i & \Delta t_i & \beta_i & \hat{u}_i^T \end{bmatrix}^T \tag{8}$$

To record whether an arc is generated naturally or with the low-thrust propulsion system, a vector of binary elements is used. Then, the complete free variable vector, $\vec{V}$, is assembled as:

$$\vec{V} = \begin{bmatrix} \vec{V}_1^T & \vec{V}_2^T & \vec{V}_3^T & \ldots & \vec{V}_N^T \end{bmatrix}^T \tag{9}$$

and describes the entire initial guess.

The constraint vector, $\vec{F}$, is constructed to enforce continuity between neighboring arcs, a positive integration time along each arc, and to fix the initial conditions at deployment. Individual components, $\vec{F}_i$, of the constraint vector capture the discontinuity between the end of the i-th arc and the beginning of the $i+1$-th arc. The vector $\vec{F}_i$ is written as:

$$\vec{F}_i = \begin{bmatrix} \vec{X}_{i,f} - \vec{X}_{i+1,0} \\ m_{i,f} - m_{i+1,0} \\ T_i + \Delta t_i - T_{i+1} \\ t_i - \beta_i^2 \end{bmatrix} \tag{10}$$

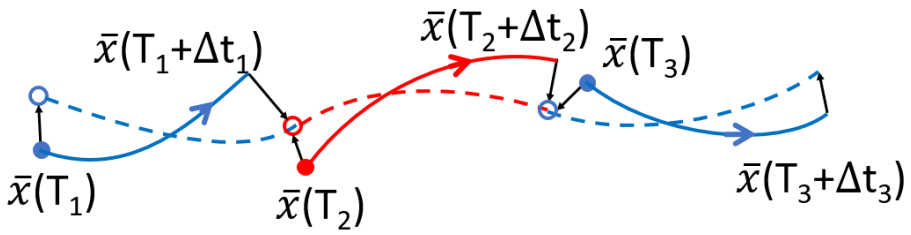

Figure 3. Illustration of the multiple shooting corrections process with natural (blue) and low-thrust (red) segments. The initial guess is represented with solid lines and the recovered trajectory is represented with a dashed line.

to maintain continuity in state, mass and time.[14] The final element of this vector constrains the integration time to retain a positive value; the slack variable, β_i is used to rewrite this requirement as an equality constraint. When constraining a finite burn to possess a minimum duration, it is useful to constrain the integration time along an arc to a value above a minimum threshold, $\Delta t_{i,\text{min}}$. In this case, the final constraint in $\vec{F}_i$ is straightforwardly modified to the equality constraint $\Delta t_i - \beta_i^2 - \Delta t_{i,\text{min}} = 0$. If the low-thrust engine is activated along the i-th arc, an additional constraint is concatenated to the end of $\vec{F}_i$. This constraint ensures that the vector, $\hat{u}_i$, describing the low-thrust maneuver is a unit vector and is written as:

$$F_{i,u} = |\hat{u}_i|^2 - 1 \tag{11}$$

An additional constraint, $\vec{F}_d$, is employed to fix the values of the initial state, epoch and mass along the trajectory equal to the deployment conditions, such that:

$$\vec{F}_d = \begin{bmatrix} \vec{X}_{1,0} - \vec{X}_{d,0} \\ m_{1,0} - m_{d,0} \\ T_1 - T_d \end{bmatrix} \tag{12}$$

where $\vec{X}_{d,0}$, $m_{d,0}$ and T_d are the initial state, mass and epoch at deployment. Then, the complete constraint vector for all N nodes is constructed as:

$$\vec{F} = \begin{bmatrix} \vec{F}_1^T & \vec{F}_2^T & \vec{F}_3^T & \dots & \vec{F}_{N-1}^T & \vec{F}_d^T \end{bmatrix}^T \tag{13}$$

In this iterative multiple shooting scheme, a Jacobian matrix is formed to reflect a linear approximation of the sensitivity of each constraint to the free variables. This matrix, $D\vec{F}(\vec{V})$, is constructed using a combination of analytical expressions and approximations via forward finite differencing. Once the Jacobian matrix is assembled, the free variables are updated at each iteration, j, via a minimum-norm update equation:

$$\vec{V}^{j+1} = \vec{V}^j - D\vec{F}(\vec{V}^j)^T \left[D\vec{F}(\vec{V}^j)\, D\vec{F}(\vec{V}^j)^T \right]^{-1} \vec{F}(\vec{V}^j) \tag{14}$$

These updates continue until the Euclidean norm of the constraint vector $\vec{F}$ converges to zero, within an appropriate tolerance.

TRAJECTORY DESIGN PROCESS

Overview

For this analysis, the SmallSat is assumed to ride as a secondary payload on a space telescope mission to a SE L2 southern quasi-halo orbit. For this sample telescope mission, the launch date is assumed to occur on January 1, 2025, and the initial deployment condition for the SmallSat is 24 hours after departing a 300km, 28.5° inclination orbit. These characteristics reflect a secondary payload that is deployed from the primary spacecraft during the transfer from the Earth vicinity and well before the primary mission maneuvers to enter the science orbit. To design a low-thrust-enabled transfer from this deployment condition to the SE L5 region, the general itinerary is described by the following three segments:

1. A departure phase from deployment in the Earth vicinity to the transfer through the SE L2 gateway, using a combination of natural and low-thrust arcs

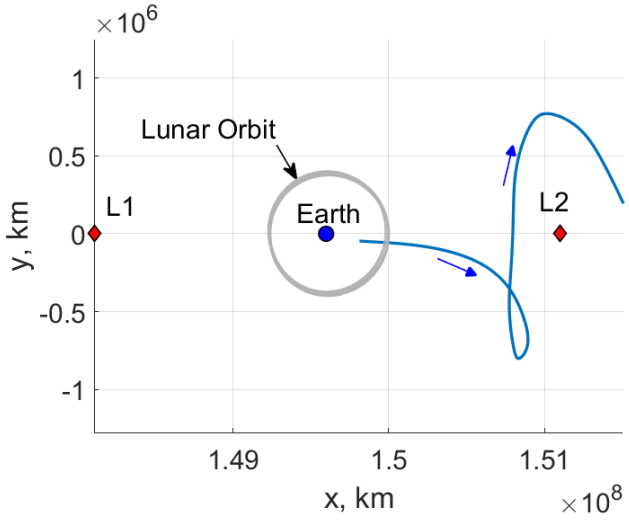

Figure 4. Natural trajectory associated with the deployment conditions and propagated for one year in a point mass ephemeris model.

2. A predominantly natural transfer segment between SE L2 and the vicinity of SE L5

3. A low-thrust-enabled insertion into a bounded science orbit around SE L5.

Using the constrained deployment condition, short low-thrust maneuvers are leveraged to explore the design space of solutions that depart through the L2 gateway. Natural unstable manifold structures associated with SE L2 halo orbits are then analyzed to identify suitable initial guesses for the transfer segment between SE L2 and SE L5. Next, short period orbits that exist near L5 in the Sun-Earth CR3BP are characterized to identify bounded motions for the science phase of the mission. Following selection of a suitable science orbit, low-thrust approach arcs are generated backwards in time and analyzed for their potential to connect to the natural manifolds of a SE L2 orbit. Poincaré mapping strategies are employed to identify arcs within both of these segments. The selected arcs are then assembled and connected with additional low-thrust segments to recover a feasible and efficient end-to-end trajectory for the SmallSat in a high-fidelity ephemeris model.

Post-Deployment and Departure from the Earth Vicinity

When propagated naturally in a point mass ephemeris model of the Sun, Earth, and Moon, the deployment conditions produce a trajectory that naturally departs through the SE L2 gateway. This trajectory is displayed in Figure 4 in a Sun-Earth rotating frame with dimensional coordinates, centered at the Sun-Earth barycenter. The trajectory of the SmallSat, propagated naturally for one year, is depicted in blue and the orbit of the Moon is colored gray. The L1 and L2 equilibrium points are located by red diamonds, while the Earth is identified by a blue filled circle. For a deployment condition near the Earth, the point mass ephemeris model is used to integrate the initial conditions as the departure phase of the trajectory may be particularly sensitive to the gravity of the Moon and the variations in the path of the Earth from a circular reference orbit.[9] Nevertheless, for this initial guess, when integrated in the point mass ephemeris model, the natural path resembles a trajectory on the stable manifold of a SE L2 halo orbit. Furthermore, the value of the Jacobi

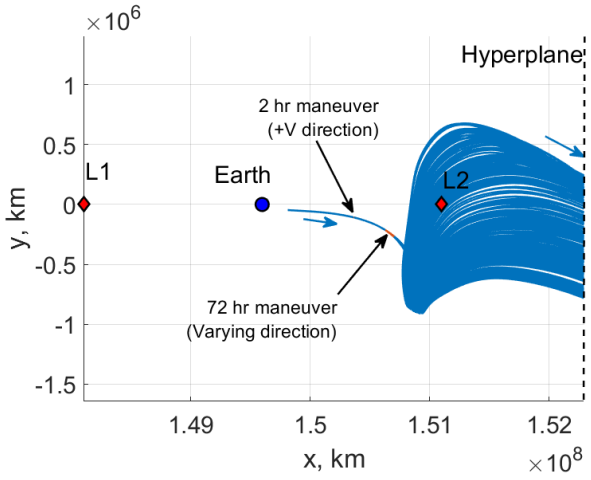

Figure 5. Sample trajectories passing through the SE L2 gateway after deployment with both natural (blue) and low-thrust (red) arcs, constructed for a SmallSat.

constant along this trajectory offers valuable insight into its characteristics, even in an ephemeris model where C_J is no longer constant along a natural solution. Following deployment, the Jacobi constant along the solution displayed in Figure 4 is approximately equal to 3.0008: lower than the Jacobi constant evaluated at SE L2, but greater than that of SE L5. This observation suggests that, while the spacecraft possesses enough energy to pass through the L2 gateway, it does not possess a sufficient energy to match the Jacobi constant of L5. Thus, to match the Jacobi constant of L5 or insert into a periodic orbit with a similar energy to L5, the value of C_J must be decreased: either through the variations that occur along a natural solution in an ephemeris model or via the application of a low-thrust maneuver.

To explore the array of solutions that pass through the SE L2 gateway, two low-thrust maneuvers are included after deployment. The first maneuver is a checkout burn with a duration of two hours in the spacecraft velocity direction with respect to the Earth. This maneuver is applied after a seven day coast period post-deployment to allow time for the spacecraft to complete system initialization activities and to ensure that the engine is working properly. Following the checkout burn, another seven day coast segment is included to allow time for additional checkouts on the spacecraft. Then, a second maneuver with a duration of 72 hours is applied in a constant direction in the spacecraft's VNC frame, defined with respect to the Earth. This maneuver leverages the sensitivity of the multi-body gravitational environment to significantly adjust the path of the spacecraft as it passes through the L2 gateway. Through analysis of a variety of thrust directions for the second maneuver, a large set of trajectories that pass through the L2 gateway are generated: a subset of these solutions is displayed in Figure 5, with coast arcs colored blue and low-thrust maneuvers displayed in red. The blue arrows indicate the general direction of motion, while the equilibrium points are displayed as red diamonds and the Earth is located by a blue filled circle. The characteristics of these trajectories as they pass through the gateway are summarized using a Poincaré mapping strategy.[9] To construct this map, a hyperplane is defined in the rotating frame at a value of the x-coordinate slightly beyond SE L2; this hyperplane appears in Figure 5 as a black dashed line. By selecting a hyperplane beyond SE L2, motion that temporarily passes through the gateway before returning the Earth vicinity is

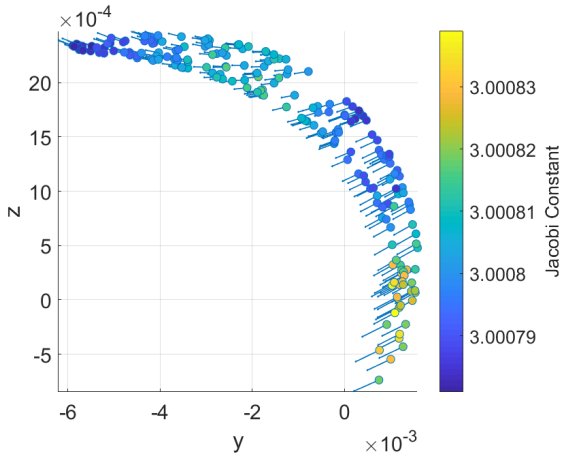

Figure 6. Poincaré map summarizing low-thrust-enabled trajectories that pass through the SE L2 gateway after deployment.

generally excluded from the data on the map. Capturing the intersection of the post-deployment arcs with this hyperplane, the corresponding map is displayed in Figure 6. The nondimensional y and z components of the map crossings in the Sun-Earth rotating frame are depicted on the horizontal and vertical axes, respectively. The $\dot{y}$ and $\dot{z}$ components of the state are represented by the horizontal and vertical components of the arrows attached to each map crossing. Finally, the value of the Jacobi constant at each map crossing is represented by the marker color, according to the colorbar on the right of the Figure 6. Using this figure as a reference, the Jacobi constant varies across the entire set of map crossings due to differences in the energy change resulting from low-thrust maneuvers in distinctly different directions, as well as gravitational perturbations. In addition, the time of flight of each trajectory represented on the map in Figure 6, measured from the initial deployment condition to its intersection with the hyperplane, is approximately equal to 150 days. These observations suggest that a brief low-thrust maneuver can produce a small change in the Jacobi constant while adjusting the spacecraft's departure through the L2 gateway – without significantly altering the flight time.

Transfer From L2 to L5

Unstable manifolds associated with periodic orbits near L2 tend to govern natural motion towards the vicinity of L5; thus, these dynamical structures are leveraged in the construction of an initial guess for this transfer segment.[15] There are several L2 orbit families that possess unstable manifolds, including the Lyapunov, halo, axial, and vertical families.[20] Unstable manifolds for several periodic orbits are rapidly generated in the CR3BP and analyzed for their Jacobi constant, out-of-plane amplitude, and flight time. Using this analysis, the L2 halo family is selected to construct a predominantly natural transfer from the L2 gateway to insertion into the L5 science orbit. These particular dynamical structures possess similar out-of-plane amplitudes and values of the Jacobi constant to candidate post-deployment trajectories as they pass through the L2 gateway. The unstable manifold structures associated with members of the halo family also posses a considerably lower time of flight to L5 when compared to the unstable manifolds of vertical and axial orbits. As an example, an unstable manifold associated with a SE L2 northern halo orbit at a Jacobi constant of 3.0008 – near the value of C_J for the deployment trajectories – is depicted in a SE rotating frame in

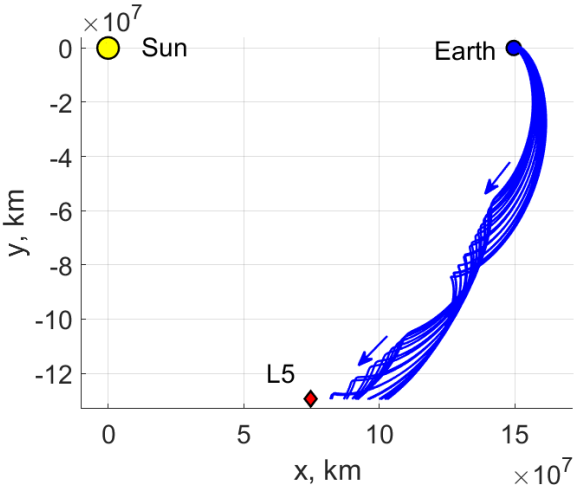

Figure 7. Unstable manifold associated with an L2 northern halo orbit at a Jacobi constant of 3.0008, capturing natural motion from the L2 gateway towards L5.

Figure 7 using dimensional coordinates. In this figure, the blue arrows represent the general direction of the flow from the Earth vicinity towards L5, while the primaries are located by filled circles and the SE L5 equilibrium point is identified by a red diamond. Analysis of this figure reveals a set of trajectories that can deliver a spacecraft from the L2 gateway to the vicinity of SE L5.

Poincaré mapping analysis is used to efficiently examine the trajectories along an unstable manifold associated with a SE L2 northern halo orbit and, then, to select a single arc for use in an initial guess. By creating a map that captures both the end of the post-deployment trajectories and the beginning of the transfer trajectories, individual arcs in each phase of the transfer are selected to reduce the discontinuity between them. To construct this map, a hyperplane defined in the SE rotating frame by $x = 1.018$ nondimensional units is used. First, an unstable manifold associated with a northern L2 halo, described by a Jacobi constant of 3.0008, is generated. The intersections of this manifold with the hyperplane are overlaid on the crossings of the post-deployment arc, previously displayed on the map in Figure 6. Then, filtering the map to only display trajectories on the unstable manifold that possess crossings close to the post-deployment arcs, produces a reduced data set depicted in Figure 8(a). This figure is constructed with the y and z components of states at each map crossing displayed on the horizontal and vertical axes, respectively. The arrow associated with each crossing represents the $\dot{y}$ and $\dot{z}$ components of the state. The color of the marker reflects the value of the Jacobi constant at each map crossings, while the color of the arrows differentiates the crossings in each segment: the post-deployment trajectories are colored in blue, and the transfer trajectories are colored in red. The black box in Figure 8(a) is expanded in Figure 8(b) to reveal a zoomed-in view of map crossings selected to select arcs within the first two segments of the trajectory. These map crossings occur at similar locations on the hyperplane with a similar value of the Jacobi constant and velocity vectors that are closely aligned; thus, only a small discontinuity between these two arcs is expected.

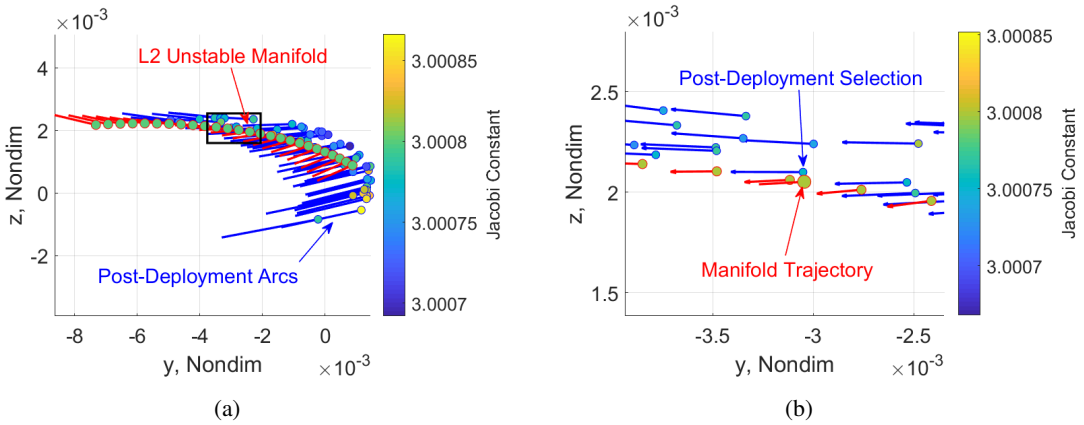

(a) (b)

Figure 8. Poincaré map summarizing crossings of the post-deployment trajectories (blue arrows) and selected SE L2 northern halo unstable manifold (red arrows) on the same hyperplane. (a) Full map view (b) Zoomed-in view of map focused on selected crossings.

Insertion to L5 Science Orbit

The final step in the initial guess construction process is the identification of a suitable science orbit near L5, as well as an insertion burn. Since L5 is located 1 AU from both the Sun and the Earth, the CR3BP offers a valuable approximation of the dynamics in this region; as a result, a rapid and informed analysis may be performed. A sample of periodic orbits along the L5 short period family is displayed in Figure 9 in the SE rotating frame using dimensional coordinates, with a configuration and color scheme that is consistent with Figure 7. The orbits displayed in Figure 9 possess Jacobi constants between 2.9996 and 2.9861. For this portion of the family, the Jacobi constant decreases as the orbits emanate away from L5 and each member has an orbital period in the rotating frame that is close to one year. Furthermore, each member of the L5 short period orbit family displayed in Figure 9 is stable, thus no stable or unstable manifolds exist in the CR3BP to generate a natural approach arc.[15] Note that the Jacobi constant for the arc selected in the L2 to L5 transfer segment is equal to approximately 3.0008. To reduce the value of the Jacobi constant to match that of a member of the SE L5 short period family and to enter a bounded orbit, a low-thrust maneuver is required. To heuristically reduce the required change in the Jacobi constant and, therefore, the propellant required to implement a low-thrust-enabled insertion, a small short period orbit at a Jacobi constant of 2.995, close to the maximum Jacobin constant along this portion of the family, is selected.

To generate an initial guess for an arc that approaches the science orbit, a long insertion maneuver is explored. The selected short period orbit is discretized into several fixed points. For each fixed point, several low-thrust trajectories are propagated backwards in time for different thrust directions, each defined as constant in a VNC frame with respect to the Earth for the duration of the maneuver.[9] Each low-thrust trajectory is propagated backwards in time for one year and then naturally propagated until the trajectory intersects a specified hyperplane. This hyperplane is defined at a fixed value of the y-coordinate in the SE rotating frame, between that of L5 and the Earth. The location of the hyperplane is constrained to lie at a great enough distance from L5 in order to capture the full duration of one year low-thrust maneuvers prior to reaching the hyperplane. Through this approach, a set of low-thrust trajectories that flow into the L5 short period orbit are generated. These trajectories are displayed in Figure 10 in the SE rotating frame using dimensional coordinates, along

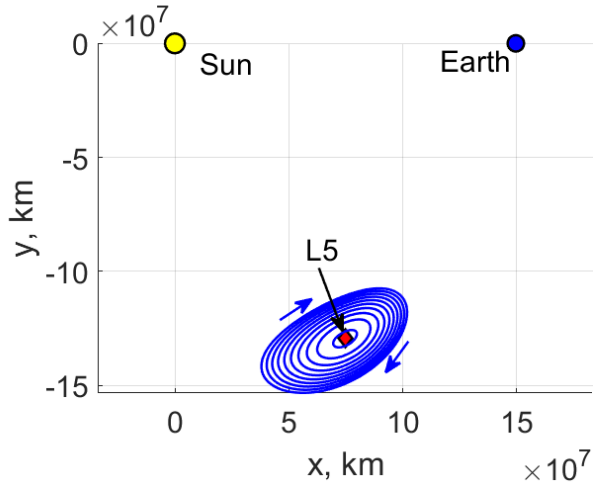

Figure 9. Periodic orbits sampled along the SE L5 short period family.

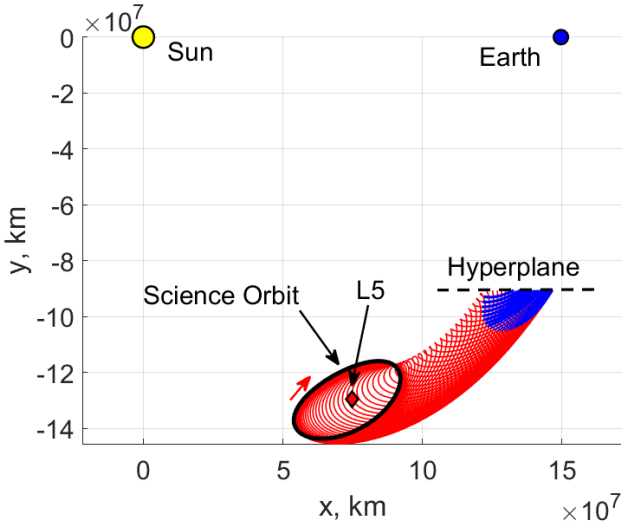

Figure 10. Low-thrust-enabled insertion into the SE L5 short period science orbit with natural arcs (blue) and low-thrust arcs (red).

with the final L5 short period science orbit. In this figure, low-thrust arcs are depicted in red and natural arcs are blue. The specified hyperplane is indicated by a black dashed line. The initial guess for the science orbit insertion arc – along with the required low-thrust maneuver – is selected to minimize the discontinuity with the end of the L2 unstable manifold arc. Once this final piece of the trajectory is selected, several revolutions of the L5 short period orbit are concatenated to the end of the initial guess to reflect multiple years of bounded motion during the science phase of the mission. Furthermore, the inclusion of these revolutions at the end of the initial guess tends to bias the multiple shooting algorithm to recover a solution that completes several revolutions around L5.

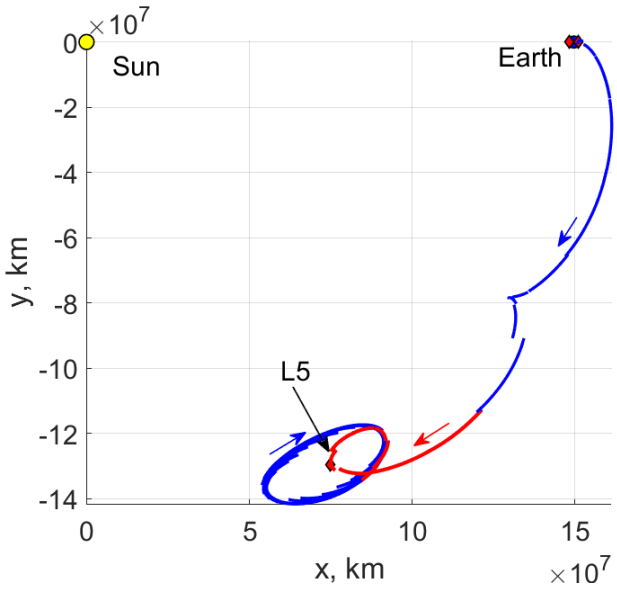

Figure 11. Initial guess for a low-thrust trajectory for a SmallSat from deployment to insertion into an L5 short period orbit. Natural arcs are displayed in blue and low-thrust maneuvers are colored red.

Recovering an End-to-End Solution

Once an initial guess is constructed using the individual arcs selected for each phase of the trajectory, the multiple shooting corrections algorithm is used to recover a continuous solution in the point mass ephemeris model. The arcs that are generated in the CR3BP – the transfer from the L2 gateway to the vicinity of L5, the L5 approach arc, and the short period orbits – must each be converted from a rotating frame to the inertial frame. This transformation is implemented via a frame rotation and dimensionalization of the states and times of the nodes by the characteristic quantities of the Sun-Earth system.[21] During this process, the nodes at the start of each arc are expressed in the inertial frame, and then integrated forward in time in the point mass ephemeris model. The resulting discontinuous initial guess for an end-to-end trajectory is displayed in Figure 11 in the SE rotating frame using dimensional coordinates. The color scheme and configuration of this figure is consistent with Figure 5. While the segments selected using dynamical system structures in the CR3BP provide a good initial guess, there are still discontinuities between neighboring arcs. The Jacobi constant evaluated along the entire initial guess, included in Figure 12, is also useful for providing additional insight into the size of these discontinuities. Each of these discontinuities are corrected using the multiple shooting algorithm.

Due to the high sensitivity of a solution that visits various regions of the Sun-Earth system, the corrections process is implemented by correcting smaller segments prior to the entire end-to-end trajectory. Recall that the initial condition for the spacecraft state, epoch, and mass are constrained to match the deployment conditions associated with a rideshare opportunity onboard a space telescope destined for SE L2. With this constraint, and the enforcement of continuity along the entire trajectory, the multiple shooting process nominally takes approximately 10 iterations for the Euclidean norm of the constraint vector to converge to zero, to within a tolerance of 1×10^{-10} nondimensional units. The recovered end-to-end trajectory for the SmallSat to reach L5 after deployment

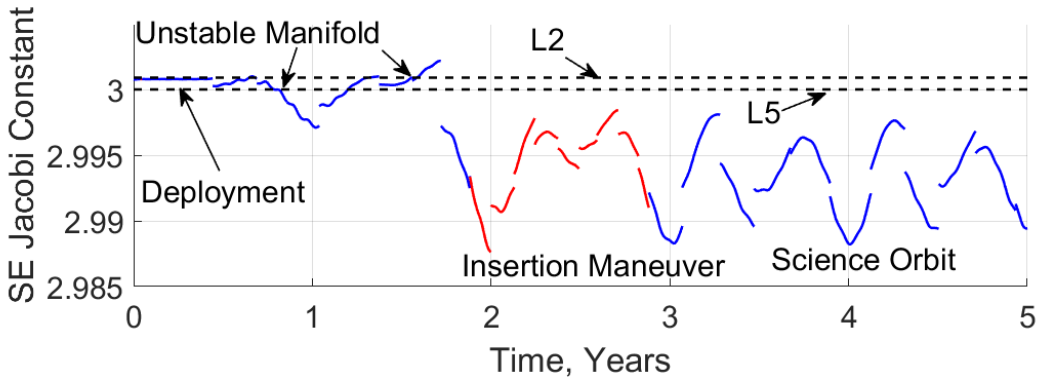

Figure 12. Sun-Earth Jacobi constant evaluated along the initial guess for the SmallSat end-to-end trajectory.

from a space telescope destined for SE L2 is displayed in Figure 13 in the SE rotating frame using dimensional coordinates. A zoomed-in view of the post-deployment phased is included in Figure 14. The color scheme and configuration of this figure is consistent with Figure 5. The time of flight for this solution, from deployment to insertion into an L5 science orbit, is 2 years and 329 days. Furthermore, this solution requires 30.427 kg of propellant, or 16.9% of the initial 180 kg wet mass of the spacecraft. Analysis of Figure 15 reveals that the recovered solution closely resembles the initial guess, supporting the value of a dynamical systems approach to trajectory design within multi-body systems for low-thrust enabled SmallSats. Furthermore, the Jacobi constant of this trajectory, evaluated in the Sun-Earth system, is portrayed in Figure 15 with low-thrust segments colored red and natural segments indicated via blue curves. Overlaid on this figure are dotted lines locating the value of the Jacobi constant at SE L2 and L5, and labels indicating the associated phase of the trajectory. In this figure, the low-thrust maneuver appears to adjust the time evolution of the value of C_J to match the values and natural oscillations that occur along a SE L5 short period orbit in the point-mass ephemeris model.

End-to-End CubeSat Trajectory Design

The outlined design process is also used to recover a point solution for the 6U CubeSat from the same deployment conditions. The 6U CubeSat spacecraft model introduces additional challenges into the trajectory design process when compared to the SmallSat spacecraft model. Namely, the CubeSat has a lower ratio of the thrust to initial wet mass, thereby lowering the available acceleration from the low-thrust engine. The CubeSat's propulsion system also possesses a lower specific impulse, which results in a less efficient use of propellant mass. However, despite these performance constraints, a similar deployment profile can be used for the CubeSat to depart through the L2 gateway. To generate a set of candidate deployment trajectories, a seven day coast arc is included immediately after deployment, followed by a two hour checkout burn in the velocity direction with respect to the Earth. After another seven day coast, a 72 hour low-thrust maneuver is included and the direction is varied to generate several candidate trajectories from post-deployment to the L2 gateway. Following the design procedure outlined in this analysis, a new initial guess is constructed and displayed in Figure 16(a) in a SE rotating frame using dimensional coordinates; low-thrust arcs are colored red and natural arcs are blue. Arrows indicate direction of motion, while the primaries are located by filled circles and L5 is identified by a red diamond. Following corrections via a

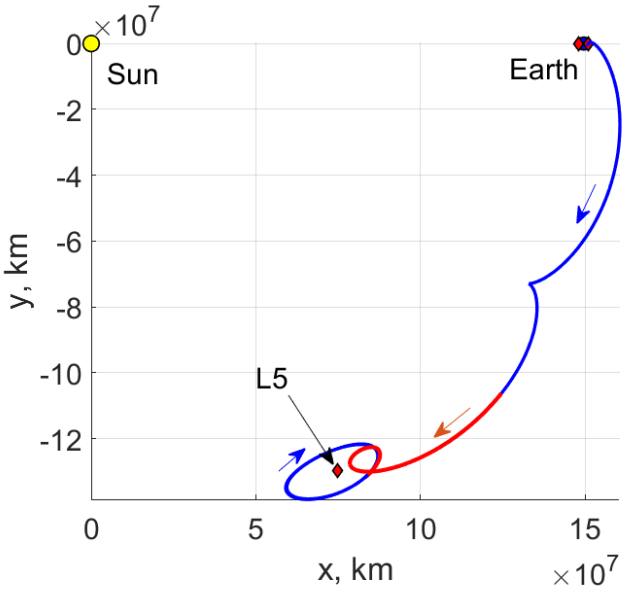

Figure 13. Continuous low-thrust trajectory for a SmallSat from deployment to insertion into an L5 short period orbit. Natural arcs are displayed in blue and low-thrust maneuvers are colored red.

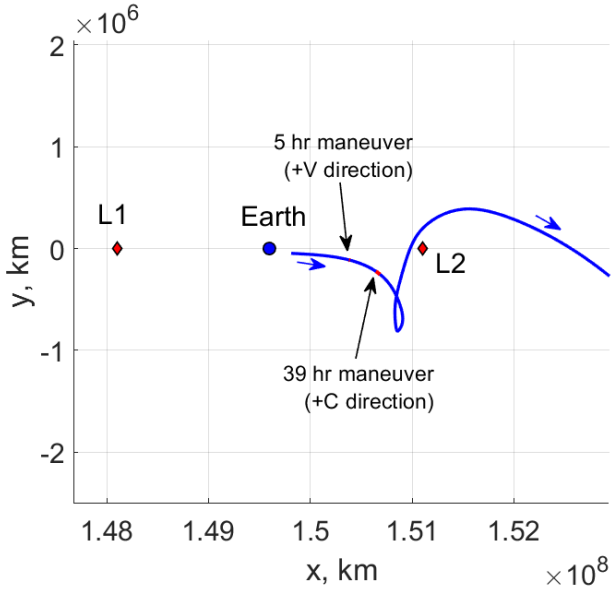

Figure 14. Zoomed-in view of post-deployment phase of SmallSat end-to-end trajectory. Natural arcs are displayed in blue and low-thrust maneuvers are colored red.

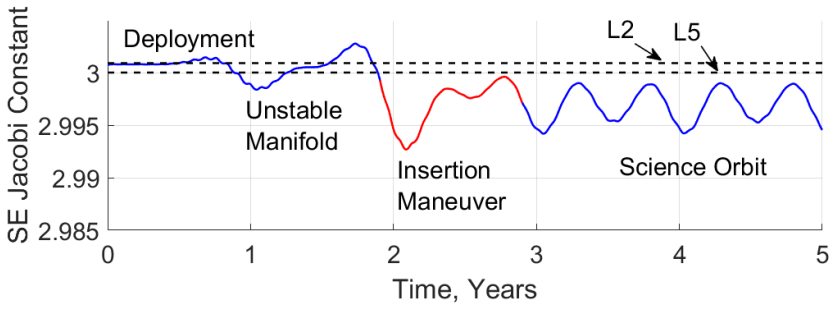

Figure 15. Sun-Earth Jacobi constant evaluated along the corrected SmallSat end-to-end trajectory.

multiple-shooting algorithm, a nearby continuous solution is uncovered, with a geometry similar to the initial guess. This end-to-end trajectory is displayed in Figure 16(b) with the same configuration and color scheme as Figure 16(a). This point solution requires a flight time of 3.49 years, with a total maneuver time of approximately 1 year and a propellant mass of 1.03 kg, that is approximately 7.4% of the initial wet mass. Both the CubeSat and SmallSat trajectories share similar characteristics in solution geometry. The characteristics of the end-to-end trajectories for each of the two spacecraft models are summarized in Table 2. In this table, the time of flight is measured from deployment to the engine shutoff for the insertion maneuver into the L5 science orbit. Analysis of the quantities in this table reveals that the time of flight for the CubeSat trajectory is longer than that of the trajectory developed for the SmallSat model. This difference in flight time may be attributed to the individual trajectories selected along L2 halo unstable manifolds during initial guess construction. Further analysis into the relationship between the application of additional finite burns may be used to reduce the flight time for the CubeSat.

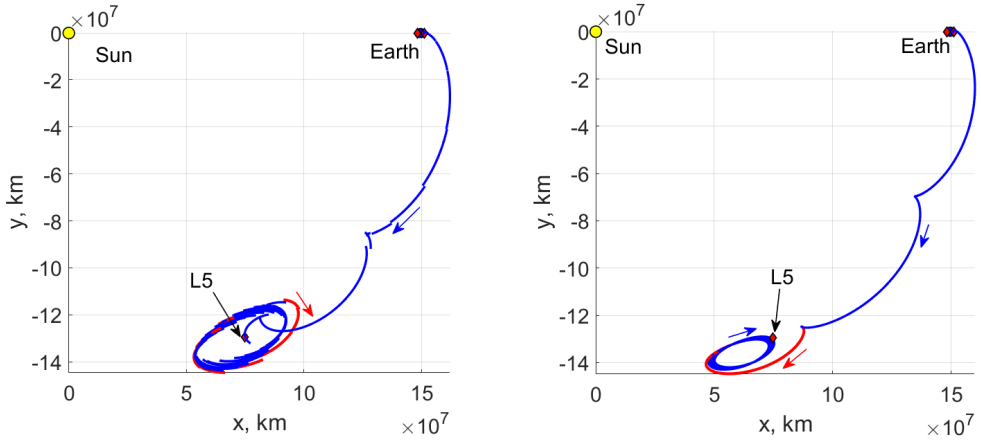

Figure 16. (a) Initial guess and (b) recovered continuous low-thrust trajectory for a 6U CubeSat from deployment to insertion into an L5 short period orbit. Natural arcs are displayed in blue and low-thrust maneuvers are colored red.

Table 2. End-to-end trajectory characteristics from initial conditions to science orbit insertion.

Characteristic	ESPA SmallSat	6U CubeSat
Time of Flight (Years)	2.899	3.490
Total Maneuver Time (Years)	1.001	1.001
Propellant Mass Used (kg)	30.428	1.030

CONCLUDING REMARKS

A dynamical systems approach to trajectory design enables the construction of an end-to-end trajectory for a small satellite to insert into an orbit around the SE L5 equilibrium point from a fixed deployment condition near the Earth. This approach is demonstrated using a sample scenario corresponding to the deployment of a small satellite from a space telescope travelling to a Sun-Earth L2 quasi-halo orbit. The trajectory design process leverages two dynamical models: the Sun-Earth CR3BP and a point-mass ephemeris model of the Sun, Earth and Moon. In the Sun-Earth CR3BP, fundamental dynamical structures offer guidance into the design process while enabling definition of a general itinerary for the trajectory. Discretizing the end-to-end trajectory into multiple segments – a post-deployment phase, a transfer phase from L2 to L5, and an insertion phase – enables construction of a complex path. Individual arcs, both natural and low-thrust, are selected within each phase using Poincaré mapping strategies. These arcs are assembled and then corrected via multiple shooting to recover a continuous solution in the point mass ephemeris model. This procedure for constructing a point solution is demonstrated for an ESPA SmallSat, with reasonable hardware constraints incorporated. Then, an additional solution is identified for a 6U CubeSat. Rapid recovery of these solutions demonstrates the value of a dynamical systems approach to trajectory design, while also indicating the potential for trajectory design to enable exciting new small satellite missions to perform targeted scientific observations for heliophysics.

ACKNOWLEDGEMENT

Part of this research was carried out at the Jet Propulsion Laboratory, California Institute of Technology, under a contract with the National Aeronautics and Space Administration and funded through the Internal Strategic University Research Partnerships (SURP) program. Part of this research was also performed at the University of Colorado Boulder. Government sponsorship acknowledged.

REFERENCES

[1] M. Akioka, T. Nagatsuma, W. Miyake, K. Ohtaka, and K. Marubashi, "The L5 Mission for Space Weather Forecasting," *Advances in Space Research*, No. 1, 2005, pp. 65–69.

[2] S. E. Gibson, A. Vourlidas, D. M. Hassler, L. A. Rachmeler, M. J. Thompson, J. Newmark, M. Velli, A. Title, and S. W. McIntosh, "Solar Physics from Unconventional Viewpoints," *Frontiers in Astronomy and Space Sciences*, Vol. 5, 2018.

[3] M. Kaiser, "The STEREO Mission: An Overview," *Advances in Space Research*, No. 8, 2005, pp. 1483–1488.

[4] M. Kaiser, T. Kucera, J. Davila, O. S. Cyr, M. Guhathakurta, and E. Christian, "The STEREO Mission: An Introduction," *Space Science Review*, 2008, pp. 5–16.

[5] A. Freeman, "Exploring our Solar System With CubeSats and SmallSats: A NASA/JPL Perspective," *The 4S Symposium*, 2018.

[6] E. Agasid, R. Burton, R. Carlino, G. Defouw, A. D. Perez, A. G. Karacalioglu, B. Klamm, A. Rademacher, J. Schalkwyk, R. Shimmin, J. Tilles, and S. Weston, "NASA State of the Art Report of Small Spacecraft Technology," 2019.

[7] N. Bosanac, F. Alibay, and J. R. Stuart, "A Low-Thrust Enabled SmallSat Heliophysics Mission to Sun-Earth L5," *IEEE Aerospace Conference*, 2018.

[8] D. Spence, E. Ehrbar, N. Rosenblad, N. Demmons, T. Roy, S. Hoffman, D. Williams, and V. Hruby, "Electrospray Propulsion Systems for Small Satellites," *27th Annual Conference on Small Satellites*, 2013.

[9] N. Bosanac, A. Cox, K. Howell, and D. C. Folta, "Trajectory Design for a Cislunar CubeSat Leveraging Dynamical Systems Techniques: The Lunar IceCube mission," *27th AAS/AIAA Space Flight Mechanics Meeting in San Antonio, Texas*, 2017.

[10] Busek, "BHT-200 Busek Hall Effect Thruster," Online; accessed October 9th 2017.

[11] Accion Systems, "TILE - Tiled Ionic Liquid Electrospray," `http://www.accion-systems.com/tile`, Online; accessed October 9th 2017.

[12] V. Szebehely, *Theory of Orbits: The Restricted Problem of Three Bodies*. London, UK: Academic Press, 1967.

[13] C. H. Acton, "Ancillary Data Services of NASA's Navigation and Ancillary Information Facility," *Planetary and Space Science*, No. 1, 1996, pp. 65–70.

[14] N. Bosanac, *Leveraging Natural Dynamical Structures to Explore Multi-Body Systems*. Ph.D. Dissertation, Purdue University, West Lafayette, IN, 2016.

[15] L. Irrgang, *Investigation of Transfer Trajectories to and from the Equilateral Libration Points L4 and L5 in the Earth-Moon System*. Ph.D. Dissertation, Purdue University, West Lafayette, IN, 2008.

[16] W. S. Koon, M. W. Lo, J. E. Marsden, and S. D. Ross, *Dynamical Systems, the Three Body Problem and Space Mission Design*. Marsden Books, 2011.

[17] M. W. Lo, "Libration Point Trajectory Design," *Numerical Algorithms*, Vol. 14, 1997, pp. 153–164.

[18] A. F. Haapala, *Trajectory Design in the Spatial Circular Restricted Three-Body Problem Exploiting Higher-Dimensional Poincare Maps*. Ph.D. Dissertation, Purdue University, West Lafayette, IN, 2014.

[19] T. A. Pavlak, *Trajectory Design and Orbit Maintenance Strategies in Multi-Body Dynamical Regimes*. Ph.D. Dissertation, Purdue University, West Lafayette, IN, 2013.

[20] D. J. Grebow, "Generating Periodic Orbits In The Circular Restricted Three-Body Problem With Applications To Lunar South Pole Coverage," Master's Thesis, Purdue University, West Lafayette, IN, 2006.

[21] T. A. Pavlak, "Mission Design Applications in the Earth-Moon System: Transfer Trajectories and Stationkeeping," Master's Thesis, Purdue University, West Lafayette, IN, 2010.